Out-of-phase oscillatory Turing patterns in a bistable reaction-diffusion system

Vladimir K. Vanag and Irving R. Epstein
Department of Chemistry and Volen Center for Complex Systems, MS 015, Brandeis University, Waltham, Massachusetts 02454, USA
(Received 4 March 2005; published 23 June 2005)

A new type of out-of-phase oscillatory Turing pattern is found in simulations of a simple two-variable model of a bistable reaction-diffusion system consisting of an autocatalytic activator reacting with a substrate that is replenished by a flow. This class of models can describe *p*H oscillators or enzymatic reactions. No Hopf instability is necessary for this type of oscillatory Turing pattern.

DOI: 10.1103/PhysRevE.71.066212 PACS number(s): 82.40.Ck, 47.54.+r, 82.33.Nq

I. INTRODUCTION

When an experimentalist encounters a spatially periodic pattern that oscillates in time so that neighboring areas are out of phase, he is likely to categorize the structure as either a standing wave [1–3] or an oscillatory Turing pattern [4,5]. Out-of-phase, spatially aperiodic, oscillatory clusters (areas having the same phase and amplitude but no intrinsic wavelength) can also be found in oscillatory media subject to periodic forcing, particularly when the forcing frequency is twice that of the natural oscillations [6–9].

Historically, the first out-of-phase oscillations were found by Huygens in 1665 in his experiments with two coupled pendulum clocks placed on a common support (see Ref. [10]). Out-of-phase oscillations can emerge if two identical excitable but nonoscillatory zero-dimensional (0D) systems (e.g., a stirred Belousov-Zhabotinsky (BZ) reaction [11,12]) are coupled via an activator species [13]. This last type of out-of-phase oscillation is similar to standing waves in 1D and 2D that arise from a wave instability [14,15]. Rhythmogenesis also occurs in a system of two diffusively coupled continuously stirred tank reactors (CSTRs) in two different steady states (SS) of the bistable chlorite-iodide reaction [16]. Two identical SS coupled via mass exchange between a pair of CSTRs give out-of-phase oscillations, in which the time delay for communication between the CSTRs plays a critical role [17]. Out-of-phase oscillations can be found as well in a system of two 0D relaxation oscillators coupled via an inhibitor species [18] (cf. Fig. 11 below). Nondiffusive coupling of bistable elements is another possible source of oscillations [19].

Prior examples of out-of-phase oscillations in spatially extended systems require a Hopf instability: an eigenvalue of the Jacobian matrix with positive real part, $\mathrm{Re}(\Lambda)$, and nonzero imaginary part, $\mathrm{Im}(\Lambda)$, at wave number $k=0$ (classical Hopf instability) for oscillatory Turing patterns and/or at $k=k_w>0$ (wave instability or Hopf instability at finite wave number [14]) for standing waves. Several theoretical works describe out-of-phase oscillatory Turing patterns resulting from Turing-Hopf or Turing-wave interactions [20–26].

Here, we report a new type of out-of-phase oscillations found computationally in a spatially extended bistable system with no oscillatory (Hopf or wave) instabilities. Most investigations of pattern formation in reaction-diffusion systems have used the oscillatory BZ, BZ-AOT [3,27], or chlorite-iodide-malonic acid (CIMA)[28] systems, each of which possesses a single steady state. The spatiotemporal behavior of bistable systems is less studied experimentally, though important works have been performed on stationary lamellar patterns and replicating spots in the ferrocyanide-iodate-sulfite (FIS) reaction-diffusion system [29–31]. The FIS system, as well as other *p*H oscillators (see Ref. [32]), may have two steady states in a CSTR.

In Sec. II we describe our models, and in Sec. III we present results obtained for different dynamical regimes (bistable, monostable, oscillatory) of the models. Section IV contains our discussion and conclusions.

II. THE MODELS

We consider a simple system of activator-depleted substrate type. Equations (1)–(3) provide a minimal description of several *p*H oscillators and enzymatic reactions.

They also resemble the mechanism of the well-known siphon, or "accumulate-and-fire," oscillator [10]

$$\mathrm{H^+ + S \rightarrow 2H^+}, \tag{1}$$

$$\mathrm{A \rightarrow H^+}, \tag{2}$$

$$\mathrm{H^+ + OH^- \rightarrow 0}. \tag{3}$$

Here, $\mathrm{H^+}$ is a proton, and S and A are substrates. [A] is constant, and $[\mathrm{H^+}]$ and [S] are the variable concentrations. Reaction (1) is autocatalytic and leads to depletion of the substrate with rate $v_1=k_1[\mathrm{H^+}][\mathrm{S}]$. Reactions (2) and (3) introduce and remove $\mathrm{H^+}$ from the system, respectively. Reaction (2) is nonlinear, and its reaction rate v_2 depends on $[\mathrm{H^+}]$ as $k_2/(K+[\mathrm{H^+}])$. This step may be an enzymatic reaction (with substrate A) that displays the usual bell-shaped dependence on $[\mathrm{H^+}]$, or an overall reaction involving a steady-state intermediate. Reaction (3) is very fast (typically diffusion controlled), and its rate depends only on the rate of $[\mathrm{OH^-}]$ inflow, $k_0[\mathrm{OH^-}]_0$, where k_0 is the reciprocal residence time of the CSTR; $[\mathrm{OH^-}]_0$ and $[\mathrm{S}]_0$ are input concentrations (concentrations in the reactor in the absence of any reaction). The ordinary differential equations that describe system (1)–(3) are

$$d[\mathrm{H^+}]/dt = k_1[\mathrm{H^+}][\mathrm{S}] + k_2/(K+[\mathrm{H^+}]) - k_0([\mathrm{OH^-}]_0 + [\mathrm{H^+}]), \tag{4}$$

$$d[\mathrm{S}]/dt = -k_1[\mathrm{H}^+][\mathrm{S}] + k_0([\mathrm{S}]_0 - [\mathrm{S}]). \quad (5)$$

We assume here that $[\mathrm{H}^+] \gg 10^{-7}$ M; otherwise, an additional term $k_0 K_w/[\mathrm{H}^+]$ should be added to Eq. (4), where $K_w = 10^{-14}$ M^2. Introducing dimensionless variables τ, s, and h defined by $t = \tau/k_1[\mathrm{S}]_0$, $[\mathrm{S}] = s[\mathrm{S}]_0$, $[\mathrm{H}^+] = h[\mathrm{S}]_0$ and parameters $\alpha = k_0/k_1[\mathrm{S}]_0$, $E = [\mathrm{OH}^-]_0/[\mathrm{S}]_0$, $\gamma = K/[\mathrm{S}]_0$, and $\beta = k_2/(k_1[\mathrm{S}]_0^3)$, Eqs. (4) and (5) are reduced to Eqs. (6) and (7)

$$dh/d\tau = sh + \beta/(\gamma + h) - \alpha(E + h), \quad (6)$$

$$ds/d\tau = -sh + \alpha(1 - s). \quad (7)$$

The combination of terms $-\alpha E$ and $\beta/(\gamma+h)$, i.e., $(\beta - \gamma\alpha E - \alpha E h)/(\gamma+h)$, serves as a negative feedback, while the sh term provides a positive feedback on h. The $\beta/(\gamma + h)$ term also serves in a sense as a delay between the positive and negative feedbacks, since it helps to keep the system near the "low h" steady state (or quasisteady state in the case of oscillations) roughly determined by $\beta/(\gamma+h) = \alpha(E+h)$, allowing the substrate that was depleted by the autocatalytic reaction to be replenished by the flow, like the water in a siphon oscillator. The characteristic time of this delay is of the order of $1/\alpha$. In the regime of relaxation oscillations, $1/\alpha$ is generally much larger than the characteristic time of autocatalysis ($\cong 1$). It is necessary that $\beta/\gamma > \alpha E$ for system (6) and (7) to ensure that h always remains positive (an analog of the condition $[\mathrm{H}^+] \gg 10^{-7}$ M).

We shall also consider a related model for pH oscillators that is applicable, for example, to the hydrogen peroxide-sulfite-ferrocyanide system [33], where the role of the substrate s is played by sulfite ion. The negative feedback is organized in a slightly different manner

$$dh/d\tau = sh - bh/(\gamma + h) + a(\varepsilon - h), \quad (8)$$

$$ds/d\tau = -sh + a(1 - s). \quad (9)$$

When $h > \gamma$, the term $-bh/(\gamma+h)$ can be approximated by $-b/\gamma$ and is equivalent to the negative feedback term $-\alpha E$ in Eqs. (6) and (7). When $h < \gamma$, the term $a\varepsilon$, the internal source of h (ε is small), corresponds to $\beta/(\gamma+h) \cong \beta/\gamma$ and the term $-bh/(\gamma+h)$ is equivalent to the terms $\beta/(\gamma+h) - \alpha E$ of Eqs. (6) and (7).

The system (6) and (7) possesses steady states I and II with large and small pH (small and large h), respectively, an oscillatory state, and a bistable regime (BS). In an appropriate parameter plane, specifically the E-α plane, these four regimes generate a cross-shaped diagram [Fig. 1(a)]. For the bistable state, which we shall focus on, typical nullclines are shown in Fig. 1(b). A simple analysis of the nullclines reveals that, for bistability to be possible, the rate of reaction (3) [term $-\alpha E$ in Eqs. (6) and (7)] must be lower order in h than the autocatalytic term (sh in our models). For example, for a quadratic autocatalytic term (like sh^2), the rate of reaction (3) can be either independent of h (zero order) or linearly dependent on h.

If we add to system (6) and (7) diffusion terms with diffusion coefficients D_h and D_S, we obtain a reaction-diffusion

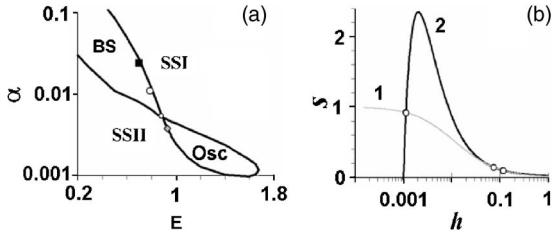

FIG. 1. Parameter diagram (a) and nullclines (b) for system (6), (7). (a) $\gamma = \beta = 1.0 \times 10^{-5}$; (b) $\alpha = 0.0121$, $E = 0.797$; line 1, $\dot{s} = 0$; line 2, $\dot{h} = 0$.

system, which we shall consider only in 1D, so the Laplacian $\Delta = \partial^2/\partial x^2$, where x is the spatial coordinate

$$\partial h/\partial\tau = sh + \beta/(\gamma + h) - \alpha(E + h) + D_h\Delta h, \quad (10)$$

$$\partial s/\partial\tau = -sh + \alpha(1 - s) + D_S\Delta s. \quad (11)$$

Along the boundary between SSI and BS, the homogeneous "high h" stationary SSII of system (10) and (11) exhibits a Turing instability for diffusion coefficient ratios D_S/D_h greater than 1 but significantly less than 10. A dispersion curve for this case is shown in Fig. 2(a), while the dependence of the maximum of $\mathrm{Re}(\Lambda)$ on D_S/D_h is shown in Fig. 2(b).

Note that the FIS experiments [29] were explained by assuming that the activator diffusion coefficient, D_h, is smaller than D_S, though this seems physically unrealistic for any actual substrate if the activator is indeed H^+. With $D_h > D_S$, no interesting patterns were obtained in models describing experiments on a spatially extended FIS system [34].

Our numerical simulations were carried out with the FLEXPDE package [35] with periodic and natural (zero flux) boundary conditions. FLEXPDE refines the triangular finite element mesh until the estimated error in any variable is less than a specified tolerance, which we chose as 10^{-4}, at every cell of the mesh. Smaller tolerances did not improve the results, and tolerances two to five times larger caused almost no changes.

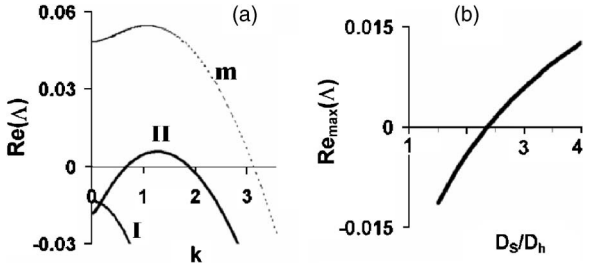

FIG. 2. (a) Dispersion curves for system (10) and (11) with $\gamma = \beta = 1.0 \times 10^{-5}$, $\alpha = 0.0121$, $E = 0.797$, $D_h = 0.01$, $D_S = 0.03$ [point marked by open circle in Fig. 1(a)]. Curves I, II, and m are real parts for steady states I ("small h"), II ("large h"), and middle state (unstable saddle point), respectively. All eigenvalues are real at all wave numbers k. (b) Dependence of maximum of $\mathrm{Re}(\Lambda)$ at $k = k_T$ [maximum of curve II in (a)] on the ratio of diffusion coefficients.

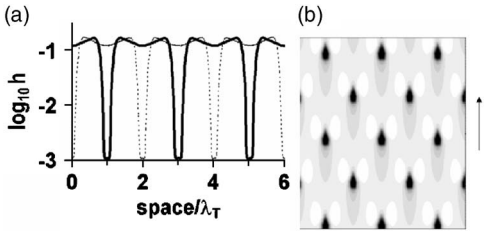

FIG. 3. Oscillatory Turing structure obtained in system (10), (11) with parameters of Fig. 2 and periodic boundary conditions. (a) Dotted and solid curves are two antiphase structures separated in time by $T/2$; (b) space-time plot. Dimensions are $6\lambda_T$ space units $\times 1000$ time units. $\lambda_T=4.89=2\pi/k_T$. Arrow shows direction of increasing time.

III. RESULTS

A. Bistable region

At the point indicated by the open circle in Fig. 1(a), the bistable spatially extended system (10) and (11) shows Turing structures that oscillate out of phase (Fig. 3). The parameter region where this behavior occurs lies close to the boundary between BS and SSI, not far from the cross point where the BS and oscillatory domains meet. Starting from the homogeneous SSII, an appropriate initial perturbation is required to generate the oscillatory Turing pattern. The 0D system exhibits no oscillations at these parameter values. The black square in the parameter diagram in Fig. 1(a) indicates a region, further from the cross point, where such oscillatory Turing patterns do not occur.

If we choose initial conditions such that part of the system is in SSI and the rest is in SSII, the front between the two states moves toward SSI, i.e., the region of SSII expands (Fig. 4). We say that the SSI is *front unstable*. Nevertheless, the homogeneous SSI is a stable state. In a set of computer experiments, we chose the ratio D_S/D_h in such a way that $\mathrm{Re}(\Lambda)<0$ [see Fig. 2(b)] to prevent Turing pattern formation behind the front. If the SSI is front unstable and SSII is Turing unstable [that is, $\mathrm{Re}(\Lambda)>0$ at some $k>0$, as in Fig. 2(a)], it seems likely that the system may produce oscillations.

System (10) and (11) can also support stationary Turing patterns at the same parameters at which oscillatory Turing patterns occur, as well in a broader range of D_S/D_h. The shape of a typical Turing pattern is shown in Fig. 5. Comparing Fig. 5 and Fig. 3(a), we see that the peaks of the

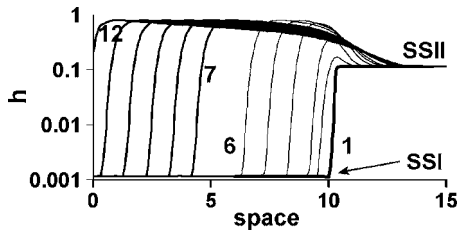

FIG. 4. Front movement in system (10), (11) at $D_h=0.01$, $D_S=0.022$ [$\mathrm{Re}(\Lambda)<0$ at $k=k_T$], $\alpha=0.0121$, $E=0.797$, zero-flux boundary conditions. Curves 1–12 correspond to times 0, 4, 8, 16, 24, 32, 48, 56, 64, 72, 80, 88, respectively.

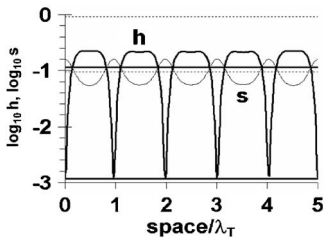

FIG. 5. Stationary Turing patterns in system (10) and (11) at $D_h=0.01$, $D_S=0.04$, $\gamma=\beta=1.0\times10^{-5}$, $\alpha=0.0121$, $E=0.797$; $\lambda_T=4.84$, two bold (h) and two thin (s) dotted horizontal lines show SSI (low h, high s) and SSII (high h, low s).

stationary Turing patterns are narrower than the peaks of the oscillatory Turing patterns. By numerically evaluating the range of D_S/D_h at which the various patterns can survive, we constructed a diagram (Fig. 6) that summarizes the multistability among the oscillatory and stationary Turing patterns as well as SSI and SSII. In a small range of negative $\mathrm{Re}(\Lambda)$, all four states can be stable, a rather rare occurrence. These results also imply that the Turing instability is subcritical, which suggests that Turing patterns may also be found in the region of SSI [Fig. 1(a)] close to the boundary between SSI and BS (see Sec. C below).

At values of $\mathrm{Re}(\Lambda)$ just above zero, transient in-phase oscillation of Turing patterns also occurs. The period of these unstable oscillations is roughly $1/\mathrm{Re}(\Lambda)$. Eventually, the in-phase oscillations transform into out-of-phase oscillations with a significantly shorter period. The period T of the out-of-phase oscillations varies with D_S/D_h [Fig. 7(b)]. Since our system has no Hopf instability at the chosen parameters, and all eigenvalues are real, we need a criterion other than the imaginary part of the eigenvalue in order to predict the period of oscillations.

One way to think about the problem is to imagine that the area around each oscillatory Turing peak, with radius $\cong\lambda_T/2$, where λ_T is the Turing wavelength or the distance between peaks, acts as a small reactor analogous to a CSTR and communicates with its neighboring peaks and reactors by diffusion. In this view, the period of oscillations should be comparable with the characteristic time of diffusion between neighboring peaks, $\tau_d\cong\lambda_T^2/D$, where D is the larger of D_h and D_S (so $D\cong D_S$). As demonstrated in Fig. 7(b), the dependences of T (curve 1) and λ_T^2/D_S (curve 2) on D_S are strik-

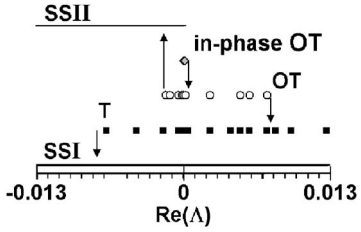

FIG. 6. Multistability between states of system (10), (11) at $\gamma=\beta=1.0\times10^{-5}$, $\alpha=0.0121$, and $E=0.797$. $\mathrm{Re}(\Lambda)$ is varied by changing D_S at $D_h=0.01$. OT, oscillatory out-of-phase Turing patterns; T, stationary Turing patterns; in-phase OT, unstable oscillatory in-phase Turing patterns. Arrows show transitions between states.

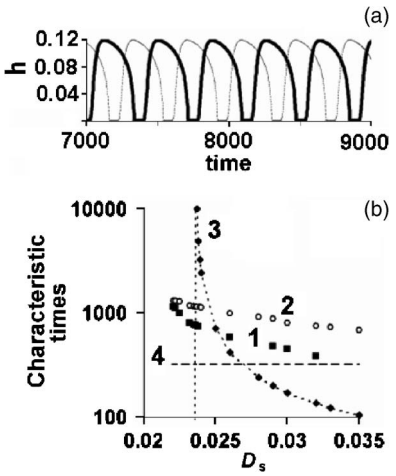

FIG. 7. (a) Oscillations at two neighboring Turing peaks (separated by $\lambda_T=5.0$) in system (10), (11) at $\beta=\gamma=1.0\times10^{-5}$, $E=0.797$, $\alpha=0.0121$, $D_h=0.01$, $D_S=0.032$. (b) (curve 1) Period of oscillations for out-of-phase Turing patterns; (curve 2) λ_T^2/D_S; (curve 3) $1/\mathrm{Re}(\Lambda)$; (curve 4) calculated minimum time for out-of-phase oscillations. Vertical line corresponds to value of D_S at which $\mathrm{Re}(\Lambda)=0$.

ingly similar, which suggests that the diffusion time λ_T^2/D_S plays a significant role in the out-of-phase oscillations.

The maximum value of T, which occurs at the smallest D_S, coincides well with the corresponding value of λ_T^2/D_S. The minimum T, at the largest D_S, is in good agreement with the "minimum" period of oscillations, T_{min}, shown as curve 4. This minimum time is calculated as a sum of four time intervals for the 0D system (6), (7): (i) the characteristic time for the SSI→SSII transition that starts when parameter α (or E) reaches the boundary between BS and SSII; (ii) the relaxation time $1/\alpha$ after the sharp SSI→SSII transition; (iii) the characteristic time for the SSII→SSI transition, when parameter α (or E) reaches the boundary between BS and SSI; (iv) the relaxation time $1/\alpha$ after the sharp II→I transition. As seen in Fig. 7(b), $T_{min}<T<\lambda_T^2/D_S$. This relation holds for the entire region along the boundary between BS and SSI and between the cross point and the filled square in Fig. 1(a).

B. Oscillatory region

We also examined the system behavior in the oscillatory region along the boundary between SSII and the oscillatory domain, since this region is a continuation of the region in the BS domain studied above. For this region, the scenario of pattern changes [again we varied D_S and used $\mathrm{Re}(\Lambda)$ as the bifurcation parameter] is quite different [Fig. 8(b)]. At the most positive $\mathrm{Re}(\Lambda)$, stationary Turing patterns are observed. In-phase oscillatory Turing patterns succeed these stationary Turing patterns at smaller $\mathrm{Re}(\Lambda)$. At still smaller $\mathrm{Re}(\Lambda)$, chaotic patterns emerge. Finally, at very small values of $\mathrm{Re}(\Lambda)$, out-of-phase oscillatory Turing patterns develop [see Fig. 8(a)]. No multi- or bistability between patterns was found, though homogeneous bulk oscillations occur at all $\mathrm{Re}(\Lambda)$. The same sequence of patterns was found for Turing-Hopf

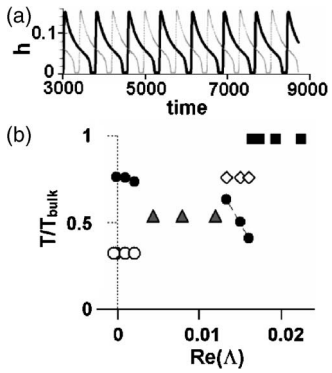

FIG. 8. (a) Oscillations at two neighboring Turing peaks (separated by $\lambda_T=6.1$) in system (10), (11) at $\beta=\gamma=1.0\times10^{-5}$, $\alpha=0.0038$, $E=0.93$, $D_h=0.01$, $D_S=0.015$. (b) $\alpha=0.0038$, $E=0.93$; open circles, triangles, open rhombs, and squares represent out-of-phase oscillatory Turing patterns, chaotic patterns, in-phase oscillatory Turing patterns, and stationary Turing patterns, respectively (they have no relation to the ordinate axis); filled circles (●), T/T_{bulk}, relate to the vertical axis; $T_{bulk}=1018$.

interaction in the Oregonator [21] and Brusselator [36] models.

A surprising feature of our model is that the period of oscillation of the Turing patterns does not equal the period of bulk oscillation, T_{bulk}, for the corresponding 0D system, but is approximately 0.5 T_{bulk} for in-phase oscillations and $\cong0.75$ T_{bulk} for out-of-phase oscillations. Since out-of-phase oscillatory Turing patterns in the oscillatory and BS domains are quite similar, we suggest that out-of-phase oscillations in the oscillatory domain do not arise from a Turing-Hopf interaction, but from the same phenomenon that causes the oscillations in the BS domain. Consequently, the period of these oscillations is unrelated to the frequency of bulk oscillations. On the other hand, the in-phase oscillations probably do reflect the bulk frequency and occur at the subharmonic $T_{bulk}/2$. The chaotic behavior at intermediate values of $\mathrm{Re}(\Lambda)$ may be a result of interaction between two quite different frequencies.

C. SSI region

As we pointed out in Sec. A, the Turing instability of SSII in the BS region close to the SSI region is subcritical. For this reason, we anticipate that stationary Turing patterns [Fig. 9(c)] can be found in the monostable region SSI close to the boundary with the BS region, despite the fact that the homogeneous SSI has no Turing instability [see the dispersion curve and nullclines in Figs. 9(c) and 9(a), respectively]. Close to the boundary with the BS region, SSI is excitable [Fig. 9(b)] and a sufficiently large perturbation can transform SSI to SSII for some finite time interval. During this time, Turing patterns can develop. Turing patterns in this region can also be obtained by starting from a previously formed stationary Turing pattern in the BS region and smoothly varying the parameter E (or α) to reach the SSI region.

D. Model (8), (9)

To extend our analysis to other bistable systems, we examined the related system (8), (9) augmented with diffusion

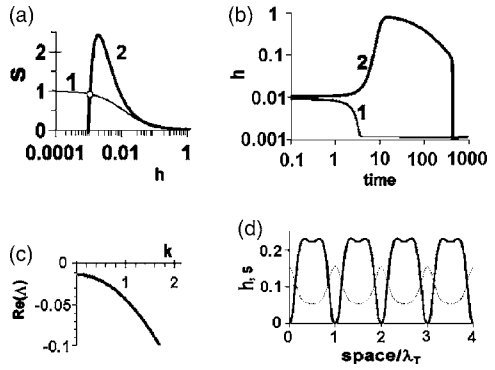

FIG. 9. Features of SSI of system (10), (11) at $\alpha=0.121$, $\beta=\gamma=10^{-5}$, $E=0.81$; (a) nullclines; (b) excitability: (curve 1) small perturbation $h_0=8h_{SS}$, $s_0=s_{SS}$; (curve 2) large perturbation $h_0=9h_{SS}$, $s_0=s_{SS}$; $h_{SS}=1.1287\times10^{-3}$, $s_{SS}=0.914\,68$. (c) dispersion curve, Re(Λ), at $D_h=0.01$ and $D_S=0.05$, Im(Λ)=0 at all k; (d) stationary Turing patterns, h=solid line, s=dotted line.

terms $D_h\Delta h$ and $D_S\Delta s$. Similar to the above results, a region of out-of-phase oscillatory Turing patterns is found in the BS domain close to the boundary between the SSI and BS regions and to the cross point of the parameter diagram (Fig. 10). The period of oscillation also shows a strong dependence on the ratio D_S/D_h. The Turing instability is again subcritical, and out-of-phase oscillatory Turing patterns can arise at negative Re(Λ). One example of such oscillations is shown in Fig. 11(a).

IV. DISCUSSION AND CONCLUSIONS

We have found a new mechanism for out-of-phase oscillatory Turing patterns in spatially extended systems. The two previously studied mechanisms for out-of-phase oscillatory Turing patterns require a Hopf instability [20,25]. De Wit *et al.* explain this spatiotemporal behavior as a resonance between a subharmonic Hopf mode and a Turing mode ("subHT mode") [20]. Yang *et al.* [25] explain the same behavior by using the dependence on the wave number k of the Floquet multipliers, $\mu(k)$, associated with the limit cycle. If $\mu(k)$ reaches 1 at wave number $k=k_T/2$, oscillatory out-of-phase Turing patterns with doubled wavelength $2\lambda_T$ (corresponding to the wave number $k_T/2$) should occur. In our bistable system, there is no Hopf instability and no limit cycle.

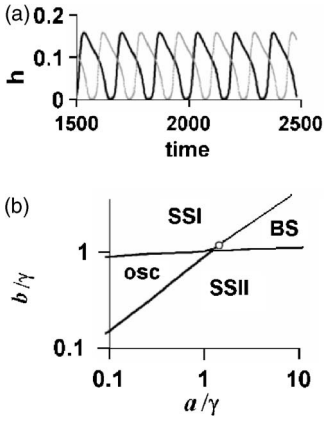

FIG. 10. (a) Oscillations at two neighboring Turing peaks (separated by $\lambda_T=21.9$) in spatially extended system (8), (9) at $a=0.029$, $b=0.0232$, $\gamma=0.02$, $\varepsilon=0.002$, $D_h=0.4$, and $D_S=1$. (b) Parameter diagram for system (8), (9) at $\gamma=0.02$, $\varepsilon=0.002$. Behavior is sensitive to the ratios a/γ and b/γ and is almost independent of small ε. Open circle marks an area where oscillatory out-of-phase Turing patterns are found.

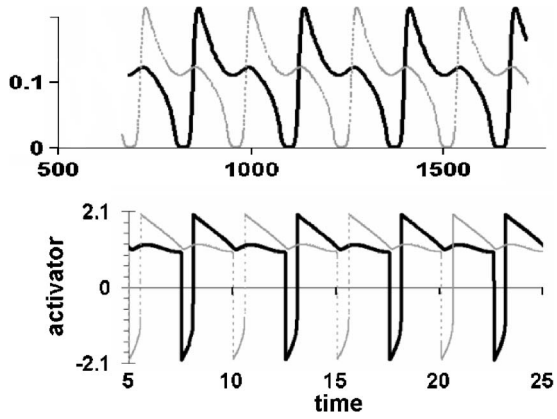

FIG. 11. Comparison of out-of-phase (a) oscillatory Turing patterns at two neighboring Turing peaks (separated by $\lambda_T=24$) in spatially extended system (8) and (9) with $a=0.029$, $b=0.0232$, $\gamma=0.02$, $\varepsilon=0.002$, $D_h=0.49$, and $D_S=1$ and (b) oscillations in inhibitory coupled 0D FitzHugh–Nagumo (FHN) systems studied in Ref. [18]: $du_{1,2}/dt=(1/\varepsilon)[v_{1,2}-u_{1,2}{}^3/3+u_{1,2}]$, $dv_{1,2}/dt=A-u_{1,2}-C(v_{1,2}-v_{2,1})$, where u is activator, v is inhibitor, subscripts 1 and 2 refer to FHN systems 1 and 2, respectively, $A=0.98$, $C=0.2$, $\varepsilon=0.0009$.

Based on the limited set of bistable systems we have investigated, we can formulate the following tentative criteria for out-of-phase oscillations of Turing patterns in a bistable system: (1) SSII is Turing unstable; (2) SSI is front unstable; (3) the system is close to the oscillatory region and to the cross point of the cross-shaped diagram; (4) the SSI$\rightarrow$SSII transition is autocatalytic.

Intuitively, we explain the oscillatory behavior as a result of diffusive coupling (with an associated time delay) of identical small "reactors" separated in space by the Turing wavelength and leading to rhythmogenesis. As we noted above, coupling of two relaxation FitzHugh–Nagumo (FHN) steady-state subsystems [see the captions to Fig. 11(b) and Ref. [18]], via the inhibitor in FHN rather than the substrate in our models, can lead to out-of-phase oscillations. We recalculated the FHN system and found out-of-phase oscillations that strikingly resemble the out-of-phase oscillations in our spatially extended systems (8), (9) or (10), (11) (Fig. 11). The comparison of Figs. 11(a), 11(b) (actually a comparison of a spatially extended system with two coupled 0D systems) would be even more compelling if out-of-phase oscillations were found for coupled 0D systems (6), (7) or (8), (9) at the same parameters at which we obtain out-of-phase oscillations in the spatially extended 1D systems. A detailed linear stability analysis of such coupled four-variable (s_1,h_1,s_2,h_2) systems with additional mass exchange terms $k_h(h_2-h_1)$ and

$k_S(s_1-s_2)$ shows no such oscillatory solution, at least of the supercritical type. We also searched for oscillations in these coupled systems by direct simulation with large perturbation, but no subcritical Hopf instability was found. It is likely that explicit introduction of a time delay, analogous to that provided by diffusion in the spatially extended systems, is necessary to obtain oscillations in these coupled reactor systems.

Although in setting up our model we have identified h with H^+, the role of h can be played by any autocatalytic species. For example, out-of-phase pigment patterns on the shell of a mollusk (sea snail) have been explained using activator-depleted substrate (with additional long-range inhibitor) type equations [37] analogous to Eqs. (6), (7) or (8), (9). When h is a large macromolecule, the relation $D_S > D_h$ can easily be fulfilled. Even when h is a proton, if reactions (1)–(3) proceed in a buffered medium or in a medium containing negatively charged polymers to which H^+ can be bound (immobilized), the effective diffusion of protons may be slower than that of the substrate.

Turing patterns oscillating in phase were found recently in the BZ-AOT system [21], and there are several experiments on standing waves in reaction-diffusion systems [2,3]. To the best of our knowledge, there is no experiment demonstrating out-of-phase oscillatory Turing patterns in reaction-diffusion systems. It is worth noting, however, Perraud *et al.*'s study of the CIMA reaction in 1D [5], where a single small area (point) emitted waves (rather than stationary patterns) out of phase to the left and to the right. It can be difficult to distinguish between standing wave patterns and out-of-phase oscillatory Turing patterns in an experiment, though theoretically this difference is evident, for example, from the dispersion curve. We emphasize the distinction between these two types of pattern in Fig. 12, in which the differences are clearly seen. The maxima and minima in standing waves are separated by very thin nodal lines. If we superpose two antiphase snapshots of a standing wave, they should cover the entire area. The maxima and minima in oscillatory Turing patterns are separated by a rather broad quiescent band of thickness λ_T, and a superposition of antiphase snapshots does not cover the entire area.

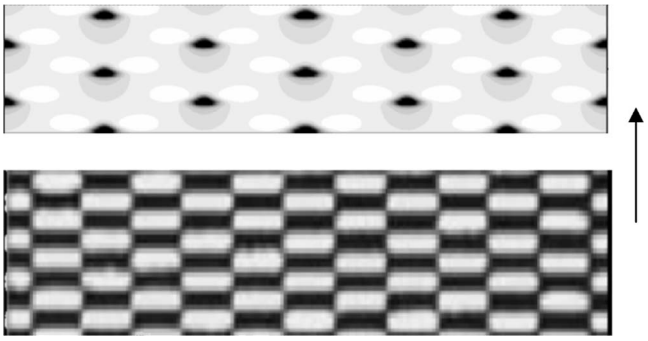

FIG. 12. Space-time plots of out-of-phase oscillatory Turing patterns [upper panel, from Fig. 3(b)] and standing waves (lower panel, from Ref. [38]). Arrow shows direction of increasing time.

With this work, there now exist three different mechanisms by which out-of-phase oscillatory Turing patterns may arise. We anticipate that experimental evidence of each of these will emerge soon.

ACKNOWLEDGMENT

This work was supported by Grant No. CHE-0306262 from the National Science Foundation.

[1] M. Bertram, C. Beta, M. Pollmann, A. S. Mikhailov, H. H. Rotermund, and G. Ertl, Phys. Rev. E **67**, 036208 (2003).
[2] S. Jakubith, H. H. Rotermund, W. Engel, A. von Oertzen, and G. Ertl, Phys. Rev. Lett. **65**, 3013 (1990).
[3] V. K. Vanag and I. R. Epstein, Phys. Rev. Lett. **87**, 228301 (2001).
[4] Z. Fei, B. J. Green, and J. L. Hudson, J. Phys. Chem. B **103**, 2178 (1999).
[5] J.-J. Perraud, A. De Wit, E. Dulos, P. De Kepper, G. Dewel, and P. Borckmans, Phys. Rev. Lett. **71**, 1272 (1993).
[6] B. Marts, K. Martinez, and A. L. Lin, Phys. Rev. E **70**, 056223 (2004).
[7] V. Petrov, Q. Ouyang, and H. L. Swinney, Nature (London) **388**, 655 (1997).
[8] V. K. Vanag, A. M. Zhabotinsky, and I. R. Epstein, J. Phys. Chem. A **104**, 11566 (2000).
[9] V. K. Vanag, A. M. Zhabotinsky, and I. R. Epstein, Phys. Rev. Lett. **86**, 552 (2001).
[10] A. Pikovsky, M. Rosenblum, and J. Kurths, *Synchronization. A Universal Concept in Nonlinear Sciences* (University Press, Cambridge, 2001).
[11] B. P. Belousov, in *Collection of Short Papers on Radiation Medicine* (Medgiz, Moscow, 1959), 145–152.
[12] A. M. Zhabotinsky, Dokl. Akad. Nauk SSSR **157**, 392 (1964).
[13] J. J. Tyson, Ann. N.Y. Acad. Sci. **316**, 279 (1979).
[14] M. C. Cross and P. C. Hohenberg, Rev. Mod. Phys. **65**, 851 (1993).
[15] V. K. Vanag and I. R. Epstein, J. Chem. Phys. **119**, 7297 (2003).
[16] M. Boukalouch, J. Elezgaray, A. Arneodo, J. Boissonade, and P. De Kepper, J. Phys. Chem. **91**, 5843 (1987).
[17] R. Holz and F. W. Schneider, J. Phys. Chem. **97**, 12239 (1993).
[18] E. I. Volkov, M. N. Stolyarov, A. A. Zaikin, and J. Kurths, Phys. Rev. E **67**, 066202 (2003).
[19] V. In, A. R. Bulsara, A. Palacios, P. Longhini, A. Kho, and J. D. Neff, Phys. Rev. E **68**, 045102(R) (2003).
[20] A. De Wit, D. Lima, G. Dewel, and P. Borckmans, Phys. Rev. E **54**, 261 (1996).
[21] A. Kaminaga, V. K. Vanag, and I. R. Epstein, J. Phys. Chem. **122**, 174706 (2005).
[22] Yu. A. Logvin, T. Ackemann, and W. Lange, Europhys. Lett. **38**, 583 (1997).
[23] M. Meixner, A. De Wit, S. Bose, and E. Schöll, Phys. Rev. E **55**, 6690 (1997).
[24] L. Yang and I. R. Epstein, Phys. Rev. Lett. **90**, 178303 (2003).

[25] L. Yang, A. M. Zhabotinsky, and I. R. Epstein, Phys. Rev. Lett. **92**, 198303 (2004).
[26] L. F. Yang, M. Dolnik, A. M. Zhabotinsky, and I. R. Epstein, J. Chem. Phys. **117**, 7259 (2002).
[27] V. K. Vanag and D. V. Boulanov, J. Phys. Chem. **98**, 1449 (1994).
[28] I. Lengyel and I. R. Epstein, Science **251**, 650 (1991).
[29] K. J. Lee, W. D. McCormick, Q. Ouyang, and H. L. Swinney, Science **261**, 192 (1993).
[30] K. J. Lee, W. D. McCormick, J. E. Pearson, and H. L. Swinney, Nature (London) **369**, 215 (1994).
[31] K. J. Lee and H. L. Swinney, Phys. Rev. E **51**, 1899 (1995).
[32] I. R. Epstein and J. A. Pojman, *An Introduction to Nonlinear Chemical Dynamics* (Oxford University Press, New York, 1998).
[33] G. Rábai, K. Kustin, and I. R. Epstein, J. Am. Chem. Soc. **111**, 3870 (1989).
[34] K. J. Lee and H. L. Swinney, Int. J. Bifurcation Chaos Appl. Sci. Eng. **7**, 1149 (1997).
[35] FLEXPDE, http://www.pdesolutions.com/flexpde.htm (2001).
[36] L. Yang, unpublished (2005).
[37] H. Meinhardt, Physica D **199**, 264 (2004).
[38] A. M. Zhabotinsky, M. Dolnik, and I. R. Epstein, J. Chem. Phys. **103**, 10306 (1995).